

Simple General-Model Pseudopotential

V. Veljković and I. Slavić

Department of Physics, Boris Kidrič Institute of Nuclear Science, Belgrade, Yugoslavia

(Received 25 April 1972)

We propose a simple general-model pseudopotential, which is in good agreement with the real potential of metal ions, especially in the range $q \leq 2k_F$.

Interaction between ions and conduction electrons in metals occurs through the central symmetric nonlocal pseudopotential $w(r)$.¹ Sham² has indicated that the nonlocal pseudopotential can be replaced by an effective local potential having the advantage of considerably simplifying the computations. The aim of this work was to find a model local pseudopotential which could give good real-potential approximations for all simple metals.

Considering the metal potential structure we have concluded that it would be interesting to unify the Coulomb potential which occurs due to the Ze core and the potential component which arises from the Pauli repulsion exerted by the bound electrons. We have found that the following mathematical form was the most suitable to describe the known potential structure, i.e., to favor the Coulomb component in the range of small wave numbers and, at the same time, to change it by further decreasing the oscillating potential in the range of large wave numbers:

$$\langle \vec{k} + \vec{q} | w | \vec{k} \rangle = \beta_1 \sin(2\pi\beta_2\eta) / 2\pi\eta, \quad (1)$$

where β_1 and β_2 , at the first step, are the two adjustable parameters, and $\eta = q/2k_F$, with q a wave number and k_F the corresponding Fermi momentum. The parameters β_1 and β_2 are fitted to the form-factor data given by Animalu and Heine³ based on the Heine-Abarenkov model potential.⁴ From the known relation valid for all forms of the local potential in which the Coulomb potential is included, we have

$$\lim_{q \rightarrow 0} \langle \vec{k} + \vec{q} | w | \vec{k} \rangle = \frac{2}{3} \hbar^2 k_F^2 / 2m^* = \frac{2}{3} E_F, \quad (2)$$

where E_F is the Fermi energy. On the other hand, from Eq. (1) we obtain the following relation:

$$\lim_{q \rightarrow 0} \langle \vec{k} + \vec{q} | w | \vec{k} \rangle = \lim_{\eta \rightarrow 0} \beta_1 \beta_2 \frac{\sin(2\pi\beta_2\eta)}{2\pi\beta_2\eta} = \beta_1 \beta_2. \quad (3)$$

Comparing Eqs. (2) and (3) we find that

$$\beta_1 \beta_2 = \frac{2}{3} E_F. \quad (4)$$

The conclusion is that in Eq. (1) only β_1 should be

fitted while β_2 , according to Eq. (4), can be found. The results for the parameters β_1 and β_2 , found in this way for 24 elements, are shown in Table I. Some representative form factors computed from Eq. (1) are shown in Table II. The errors

TABLE I. Proposed model pseudopotential parameters computed from the fit by the Heine-Abarenkov model potential.

Metals	β_1 Ry	β_2 $\times 10^{-2}$
Li	- 2, 9741	5, 8471
Na	- 2, 5830	5, 6121
K	- 2, 0297	5, 7895
Rb	- 2, 2900	4, 8009
Cs	- 2, 2977	4, 3583
Be	- 9, 6093	7, 3415
Mg	- 5, 3679	6, 5139
Ca	- 3, 2853	6, 9808
Ba	- 2, 2670	7, 9149
Zn	- 6, 9613	6, 0589
Cd	- 6, 2427	5, 8838
Hg	- 6, 4095	5, 4115
Al	- 7, 8967	7, 2638
Ga	- 8, 0517	6, 3775
In	- 6, 8243	6, 2090
Tl	- 6, 9242	5, 7653
Si	- 9, 2737	6, 6108
Ge	- 8, 6594	6, 5247
Sn	- 7, 6781	6, 5322
Pb	- 7, 7704	5, 9826
Sb	- 8, 3321	6, 4614
Bi	- 7, 9886	6, 0574
Se	-10, 0407	6, 3128
Te	- 8, 7329	6, 4736

TABLE II. Some illustrative form factors computed by the model pseudopotential proposed in this work.

q/k_F	Formfactors in rydberg					
	Sodium $\beta_1 = -2.5830$ $\beta_2 = 5.7895 \times 10^{-2}$	Potassium $\beta_1 = -2.0297$ $\beta_2 = 5.7895 \times 10^{-2}$	Barium $\beta_1 = -2.2670$ $\beta_2 = 7.9149 \times 10^{-2}$	Zinc $\beta_1 = -6.9613$ $\beta_2 = 6.0589 \times 10^{-2}$	Mercury $\beta_1 = -6.4095$ $\beta_2 = 5.4115 \times 10^{-2}$	Indium $\beta_1 = -6.8243$ $\beta_2 = 6.2090 \times 10^{-2}$
0,0	-0,14496	-0,11751	-0,17943	-0,42178	-0,34685	-0,42372
0,1	-0,14421	-0,11686	-0,17759	-0,41924	-0,34518	-0,42104
0,2	-0,14197	-0,11494	-0,17213	-0,41167	-0,34021	-0,41305
0,3	-0,13829	-0,11177	-0,16325	-0,39923	-0,33201	-0,39995
0,4	-0,13324	-0,10741	-0,15128	-0,38219	-0,32073	-0,38202
0,5	-0,12690	-0,10197	-0,13665	-0,36093	-0,30656	-0,35967
0,6	-0,11940	-0,09554	-0,11989	-0,33589	-0,28975	-0,33340
0,7	-0,11086	-0,08824	-0,10160	-0,30760	-0,27059	-0,30380
0,8	-0,10146	-0,08022	-0,08242	-0,27666	-0,24938	-0,27152
0,9	-0,09134	-0,07163	-0,06299	-0,24372	-0,22650	-0,23725
1,0	-0,08070	-0,06263	-0,04396	-0,20944	-0,20232	-0,20174
1,1	-0,06972	-0,05339	-0,02593	-0,17451	-0,17723	-0,16573
1,2	-0,05859	-0,04407	-0,00945	-0,13963	-0,15164	-0,12996
1,3	-0,04750	-0,03485	0,00504	-0,10546	-0,12595	-0,09515
1,4	-0,03662	-0,02587	0,01717	-0,07263	-0,10055	-0,06195
1,5	-0,02813	-0,01730	0,02669	-0,04173	-0,07584	-0,03099
1,6	-0,01620	-0,00926	0,03344	-0,01328	-0,05217	-0,00280
1,7	-0,00696	-0,00188	0,03755	0,01227	-0,02986	-0,00280
1,8	0,00146	0,00474	0,03897	0,03457	-0,00922	0,02218
1,9	0,00895	0,01051	0,03798	0,05334	0,00950	0,04358
2,0	0,01542	0,01538	0,03486	0,06840	0,02608	0,07480

are of the order 0.001 Ry in the stated interval; the general behavior for the $q > 2k_F$ range has the same trend as the "experimental" curve but the errors are about 0.01 Ry.

A comparison is also made in Fig. 1, where H denotes Harrison's curve¹ of the form factors for zinc, the dashed line gives the "experimental" form factors,³ and the solid line represents the form factors for zinc computed by the present model pseudopotential, Eq. (1). Periodic dependence of the parameter β_1 on Z is shown in Fig. 2, where the values presented correspond to those given in Table I and the Roman numerals denote the periods.

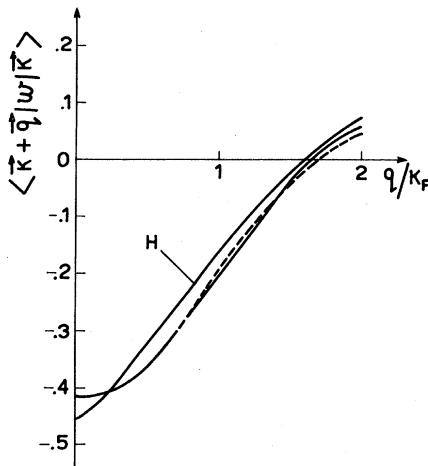


FIG. 1. Comparison of the form factors for zinc.

On the basis of the above analysis we can establish a general-model pseudopotential relation as follows:

$$\langle \vec{k} + \vec{q} | w | \vec{k} \rangle_Z = \alpha (Z - Z_0) \sin(2\pi\beta_Z \eta) / 2\pi\eta, \quad (5)$$

where

$$\beta_Z = \frac{2}{3} (E_F)_Z / \alpha (Z - Z_0) \quad (6)$$

and the coefficient

$$\alpha \approx \begin{cases} -2.500 & \text{for short and the first} \\ & \text{half of long periods,} \\ -0.625 & \text{for the second half of} \\ & \text{long periods.} \end{cases} \quad (7)$$

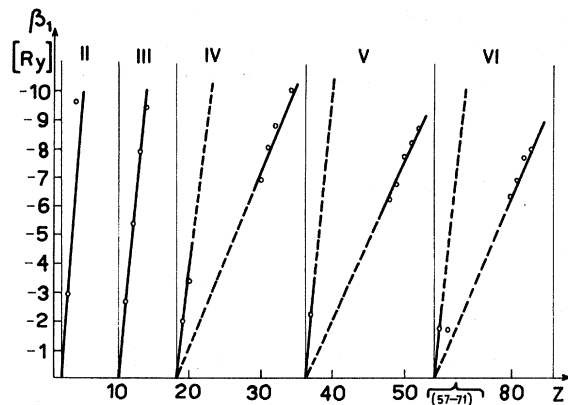


FIG. 2. Periodic dependence of the parameter β_1 on Z . The points represent the values given in Table I. Roman numerals denote periods, and the lanthanum group is truncated into one abscissa point.

Z is the atomic number, Z_0 is the inert-element atomic number that begins the period which includes the actual Z , and $(E_F)_Z$ is the corresponding Fermi energy.

The general-model pseudopotential presented enables simple computation of the form factors in the small-wave-number range which is an appreciable advantage, especially in the estimation

of electronic properties.

¹W. A. Harrison, *Pseudopotentials in the Theory of Metals* (Benjamin, New York, 1966).

²L. J. Sham, Proc. Roy. Soc., London, Ser. A **233**, 33 (1965).

³A. O. E. Animalu and V. Heine, Phil. Mag. **12**, 1249 (1965).

⁴V. Heine and I. Abarenkov, Phil. Mag. **9**, 451 (1964).

Anomalous Double Spin-Flip Raman Scattering in CdS, and a Visible Spin-Flip Laser

J. F. Scott and T. C. Damen

Bell Laboratories, Holmdel, New Jersey 07733

(Received 16 December 1971; revised manuscript received 10 March 1972)

We have observed a peak in the inelastic light scattering of CdS in high magnetic fields at an energy slightly less than twice the bound electron spin-flip energy μgH . The intensity, selection rules, field dependence, and binding energy of this process cannot be explained as second-order scattering. At very high excitation energies (≥ 1 MW/cm²) the single spin-flip scattering becomes stimulated, with a sharp threshold and high conversion efficiency.

We have examined the inelastic light-scattering spectra of CdS in high magnetic fields (40–100 kG) and have found, in addition to the $\Delta S = 1$ spin-flip scattering from bound¹ and free² electrons reported previously, a strong peak in the spectrum at an energy slightly (0.25 ± 0.05 cm⁻¹) less than twice the shift of the $\Delta S = 1$ bound electron energy μgH (7.85 cm⁻¹ at 89 kG).³ The intensity, selection rules, field dependence, and apparent binding energy of the double spin-flip process cannot be accounted for by model calculations which treat the $\Delta S = \pm 2$ scattering as second order; however, all these anomalies have been interpreted via a theory⁴ based on a simple model of the electronic interactions.

Our experiments consist of Raman scattering from CdS specimens having carrier concentrations between $n = 1 \times 10^{16}$ and 5×10^{17} cm⁻³. These were obtained from Eagle Picher and were shown by spectrochemical analysis to contain 10^{17} – 10^{18} cm⁻³ in donor concentration. The samples were illuminated with light at 4765, 5880, 4965, and 5145 Å from a 2-W argon ion laser at temperatures between 2.0 and 25°K and in magnetic fields from 40 to 100 kG. At these low temperatures all samples exhibited spin-flip scattering ($\Delta S = \pm 1$) with selection rules compatible with those calculated by Thomas and Hopfield¹ for electrons bound to neutral donors having C_{3v} site symmetry. In particular, α_{xz} , α_{xx} , and α_{xy} polarizability

components were equally strong, where Z is the direction of applied field. In contrast, the same samples exhibited only $\alpha_{xz} = \alpha_{yz}$ scattering at higher temperatures ($> 80^\circ\text{K}$), as reported earlier by Fleury and Scott.² The low-temperature scattering intensity is attributed to bound-electron spin flip, whereas the high-temperature scattering is attributed to free electrons. In addition to selection-rule differences, the free- and bound-electron spin-flip processes exhibit different linewidths and different dependences upon momentum transfer or scattering angle.⁵ The free- and bound-electron g values are very nearly the same, both lying between 1.80 and 1.86.

In the present study, we have observed, in addition to the $\Delta S = \pm 1$ spin-flip processes reported in Refs. (1) and (2), sharp lines at energies slightly less than twice the single spin-flip energy $\Delta = \mu gH$. These are shown in Fig. 1 for an $n = 1 \times 10^{16}$ cm⁻³ sample at 40 kG and 2.0°K. Significant features of the higher-energy feature are (1) its intensity is $(5 \pm 1)\%$ of that for the $\Delta S = 1$ line; (2) its selection rules are exactly the same as those for the $\Delta S = 1$ process, i.e., the relative intensity $I(\Delta S = 2)/I(\Delta S = 1)$ is independent of polarizability tensor component (5% for α_{xx} , α_{xy} , and α_{xz} ; $z \parallel \vec{H}$); (3) its frequency is given by $\omega = 2\Delta - (0.25 \pm 0.05$ cm⁻¹), where $\Delta = \mu gH = 3.52$ cm⁻¹ at 40 kG. That is, the fea-